dysfunction, can be reversed in aging by using a nutritional intervention to boost NAD^+ concentrations in SCs. Additionally, our findings suggest that NAD^+ repletion may be revealed as an attractive strategy for lengthening mammalian life span.

REFERENCES AND NOTES

1. A. J. Wagers, I. L. Weissman, *Cell* **116**, 639–648 (2004).
2. T. Kuilman, C. Michaloglou, W. J. Mooi, D. S. Peeper, *Genes Dev.* **24**, 2463–2479 (2010).
3. C. López-Otín, M. A. Blasco, L. Partridge, M. Serrano, G. Kroemer, *Cell* **153**, 1194–1217 (2013).
4. H. Yin, F. Price, M. A. Rudnicki, *Physiol. Rev.* **93**, 23–67 (2013).
5. M. Tabebordbar, E. T. Wang, A. J. Wagers, *Annu. Rev. Pathol.* **8**, 441–475 (2013).
6. Y. C. Jang, M. Sinha, M. Cerletti, C. Dall'Osso, A. J. Wagers, *Cold Spring Harb. Symp. Quant. Biol.* **76**, 101–111 (2011).
7. C. S. Fry *et al.*, *Nat. Med.* **21**, 76–80 (2015).
8. F. D. Price *et al.*, *Nat. Med.* **20**, 1174–1181 (2014).
9. I. M. Conboy *et al.*, *Nature* **433**, 760–764 (2005).
10. J. V. Chakkalakal, K. M. Jones, M. A. Basson, A. S. Brack, *Nature* **490**, 355–360 (2012).
11. P. Sousa-Victor *et al.*, *Nature* **506**, 316–321 (2014).
12. J. D. Bernet *et al.*, *Nat. Med.* **20**, 265–271 (2014).
13. B. D. Cosgrove *et al.*, *Nat. Med.* **20**, 255–264 (2014).
14. L. Liu *et al.*, *Cell Reports* **4**, 189–204 (2013).
15. M. T. Tierney *et al.*, *Nat. Med.* **20**, 1182–1186 (2014).
16. C. Cantó *et al.*, *Cell Metab.* **15**, 838–847 (2012).
17. E. Pirinen *et al.*, *Cell Metab.* **19**, 1034–1041 (2014).
18. L. Mouchiroud *et al.*, *Cell* **154**, 430–441 (2013).
19. J. Yoshino, K. F. Mills, M. J. Yoon, S. Imai, *Cell Metab.* **14**, 528–536 (2011).
20. A. P. Gomes *et al.*, *Cell* **155**, 1624–1638 (2013).
21. K. Ito, T. Suda, *Nat. Rev. Mol. Cell Biol.* **15**, 243–256 (2014).
22. M. Cerletti, Y. C. Jang, L. W. Finley, M. C. Haigis, A. J. Wagers, *Cell Stem Cell* **10**, 515–519 (2012).
23. L. R. Stein, S. Imai, *EMBO J.* **33**, 1321–1340 (2014).
24. P. Katajisto *et al.*, *Science* **348**, 340–343 (2015).
25. J. G. Ryall *et al.*, *Cell Stem Cell* **16**, 171–183 (2015).
26. T. R. Mercer *et al.*, *Cell* **146**, 645–658 (2011).
27. A. Sickmann *et al.*, *Proc. Natl. Acad. Sci. U.S.A.* **100**, 13207–13212 (2003).
28. D. J. Pagliarini *et al.*, *Cell* **134**, 112–123 (2008).
29. R. H. Houtkooper, C. Cantó, R. J. Wanders, J. Auwerx, *Endocr. Rev.* **31**, 194–223 (2010).
30. S. Sartore, L. Gorza, S. Schiaffino, *Nature* **298**, 294–296 (1982).
31. D. R. Lemos *et al.*, *Nat. Med.* **21**, 786–794 (2015).
32. E. Hara *et al.*, *Mol. Cell. Biol.* **16**, 859–867 (1996).
33. L. C. Gillet *et al.*, *Mol. Cell. Proteomics* **11**, O111.016717 (2012).
34. P. Rimmelé *et al.*, *EMBO Rep.* **16**, 1164–1176 (2015).
35. P. J. Coates *et al.*, *Exp. Cell Res.* **265**, 262–273 (2001).
36. P. J. Coates, D. J. Jamieson, K. Smart, A. R. Prescott, P. A. Hall, *Curr. Biol.* **7**, 607–610 (1997).
37. M. Artal-Sanz, N. Tavernarakis, *Nature* **461**, 793–797 (2009).
38. C. Osman, C. Merkwirth, T. Langer, *J. Cell Sci.* **122**, 3823–3830 (2009).
39. M. Fulco *et al.*, *Mol. Cell* **12**, 51–62 (2003).
40. K. P. Quinn *et al.*, *Sci. Rep.* **3**, 3432 (2013).
41. E. K. Nishimura, S. R. Granter, D. E. Fisher, *Science* **307**, 720–724 (2005).
42. C. D. Folmes, P. P. Dzeja, T. J. Nelson, A. Terzic, *Cell Stem Cell* **11**, 596–606 (2012).
43. C. Cantó, K. J. Menzies, J. Auwerx, *Cell Metab.* **22**, 31–53 (2015).

ACKNOWLEDGMENTS

H.Z., D.R., K.J.M., J.A., and the EPFL have filed a provisional patent application on the use of NAD boosting to enhance SC function. We thank T. Langer for sharing the *Phb* plasmids; S. Wang and M. Knobloch for technical help in McSC and NSC experiments; H. Li, L. Mouchiroud, P. Moral Quiros, and all members of the Auwerx and Schoonjans groups for helpful discussions; and the EPFL histology and flow cytometry core facilities for technical assistance. H.Z. is the recipient of a doctoral scholarship from the China Scholarship Council and a fellowship from CARIGEST SA. D.D. was supported by a fellowship from Associazione Italiana per la Ricerca sul Cancro. K.J.M. is supported by the University of Ottawa and the Heart and Stroke Foundation of Canada. J.A. is the Nestlé Chair in Energy Metabolism, and his research is supported by EPFL, the NIH (grant R01AG043930), Krebsforschung Schweiz/SwissCancerLeague (grant KFS-3082-02-2013), Systems X (grant SySX.ch 2013/153), and the Swiss National Science Foundation (grant 31003A-140780).

SUPPLEMENTARY MATERIALS

www.sciencemag.org/content/352/6292/1436/suppl/DC1
Materials and Methods
Figs. S1 to S6
Tables S1 to S6
References (*44*–*54*)

16 January 2016; accepted 13 April 2016
Published online 28 April 2016
10.1126/science.aaf2693

REPORTS

MOLECULAR JUNCTIONS

Covalently bonded single-molecule junctions with stable and reversible photoswitched conductivity

Chuancheng Jia,[1]* Agostino Migliore,[2]* Na Xin,[1]* Shaoyun Huang,[3]* Jinying Wang,[1] Qi Yang,[3] Shuopei Wang,[4] Hongliang Chen,[1] Duoming Wang,[4] Boyong Feng,[3] Zhirong Liu,[1] Guangyu Zhang,[4] Da-Hui Qu,[5] He Tian,[5] Mark A. Ratner,[6] H. Q. Xu,[3]† Abraham Nitzan,[7,8]† Xuefeng Guo[1,9]†

Through molecular engineering, single diarylethenes were covalently sandwiched between graphene electrodes to form stable molecular conduction junctions. Our experimental and theoretical studies of these junctions consistently show and interpret reversible conductance photoswitching at room temperature and stochastic switching between different conductive states at low temperature at a single-molecule level. We demonstrate a fully reversible, two-mode, single-molecule electrical switch with unprecedented levels of accuracy (on/off ratio of ~100), stability (over a year), and reproducibility (46 devices with more than 100 cycles for photoswitching and ~10^5 to 10^6 cycles for stochastic switching).

Rapidly growing research in nanoscience has implications for the development of computing devices, solar energy harvesting, chemical sensing (*1*–*4*), photonics and optoelectronics, biomedical electronics [such as cell-chip connections, cyborg cells (*5*), electroceuticals (*6*), and prosthetics], and biofuel cells (*7*). The development of electronic devices based on controllable molecular conduction aims to meet the urgent demand for further device miniaturization on one hand, and the need to effectively interface organic and inorganic materials for biomedical and nanoelectronic applications on the other. To this end, diverse approaches to molecular nanodevices have been proposed and have faced important issues of reproducibility and stability (*8*).

Switches are basic components of almost any electronic device. The manufacturing of reliable molecular switches is a crucial test of the possibility to use molecules as pivotal components of electronic devices. Molecular switches have been intensively investigated for two decades (*9*–*11*), but only a few studies have demonstrated unidirectional switching (namely, irreversible change) in molecular conduction (*12*–*14*), while failing to produce actual (bidirectional) conductance switching. In this work, we demonstrate a reversible molecular electrical switch that consists of a single diarylethene molecule in a junction comprising graphene electrodes.

[1]Beijing National Laboratory for Molecular Sciences, State Key Laboratory for Structural Chemistry of Unstable and Stable Species, College of Chemistry and Molecular Engineering, Peking University, Beijing 100871, P. R. China. [2]Department of Chemistry, Duke University, Durham, NC 27708, USA. [3]Department of Electronics and Key Laboratory for the Physics and Chemistry of Nanodevices, Peking University, Beijing 100871, P. R. China. [4]Institute of Physics, Chinese Academy of Sciences, Beijing 100190, P. R. China. [5]Key Laboratory for Advanced Materials and Institute of Fine Chemicals, East China University of Science and Technology, Shanghai 200237, P. R. China. [6]Department of Chemistry, Northwestern University, Evanston, IL 60208, USA. [7]Department of Chemistry, University of Pennsylvania, Philadelphia, PA 19104-6323, USA. [8]School of Chemistry, Tel Aviv University, Tel Aviv, 69978, Israel. [9]Department of Materials Science and Engineering, College of Engineering, Peking University, Beijing 100871, P. R. China.
*These authors contributed equally to this work. **†Corresponding author. Email: guoxf@pku.edu.cn (X.G.); anitzan@sas.upenn.edu (A.N.); hqxu@pku.edu.cn (H.Q.X.)**

One of the most challenging issues in fabricating reliable (namely, stable and reproducible) molecular switches is the lack of control of the properties of the molecule-electrode interface (*15*). In particular, only unidirectional optoelectronic switching (from closed and conducting to open and nonconducting diarylethene) was observed for single diarylethenes sandwiched between gold electrodes via Au–S bonds (*12*). This response was attributed to quenching of the excited state of the open molecular form in the presence of the Au electrode. We have reported the opposite unidirectional photoswitching of single diarylethenes (from the insulating open form to the conducting closed form) when they were used to bridge nanogaps between carbon electrodes [either single-walled carbon nanotubes (*13*) or graphene sheets (*14*)] because the molecule remained locked in its closed form as a consequence of the energy transfer from the photoexcited molecule to the extended π-electron system in the electrodes. This quenching effect resulted from the strong molecule-electrode couplings produced by the covalent amide linkages, which we originally used to enhance the device stability (*16*, *17*). These results have stressed the crucial importance of the molecule-electrode coupling strength in determining the device performance.

To overcome this issue, in the present study we have incorporated three methylene (CH_2) groups into each side of the molecular backbone (Fig. 1, scheme S1, and fig. S1) (*18*) in order to decrease the effective molecule-electrode coupling. Theoretical analysis suggests that this structural modification reduces the electrode-molecule coupling to a level that may avoid the quenching of the molecular excited state by the electrodes and moves the system from the Landauer regime without the CH_2 groups closer to the Coulomb blockade regime, in which the molecule is locked in either the closed or open conformation. Our calculations show narrow resonance half-widths of the transmission peaks [in correspondence to the perturbed highest occupied molecular orbital (HOMO) and lowest unoccupied molecular orbital (LUMO) energies (fig. S2)] (*18*), which amount to interfacial graphene-molecule coupling on the order of 1 meV in both open and closed forms—that is, considerably weaker than those in previous cases (*14*).

It was found that diarylethene-reconnected molecular junctions with graphene electrodes reversibly switched at a single-molecule level in a robust and reproducible way (Fig. 2); 46 devices were successfully implemented and studied. The on/off ratio was 107.1 ± 56.3 when light with different wavelengths was toggled back and forth (Fig. 2, A and B; figs. S3 to S7; and table S1) (*18*). The assignment of the open and closed molecular forms was further confirmed by means of low-temperature inelastic electron tunneling spectroscopic measurements and related theoretical analysis (figs. S9 to S12) (*18*).

Our theoretical analysis (supplementary materials, section S9.2) (*18*) shows that the HOMO of diarylethene is the only molecular orbital with energy close enough to the unbiased electrode chemical potentials to enter the electrode Fermi window

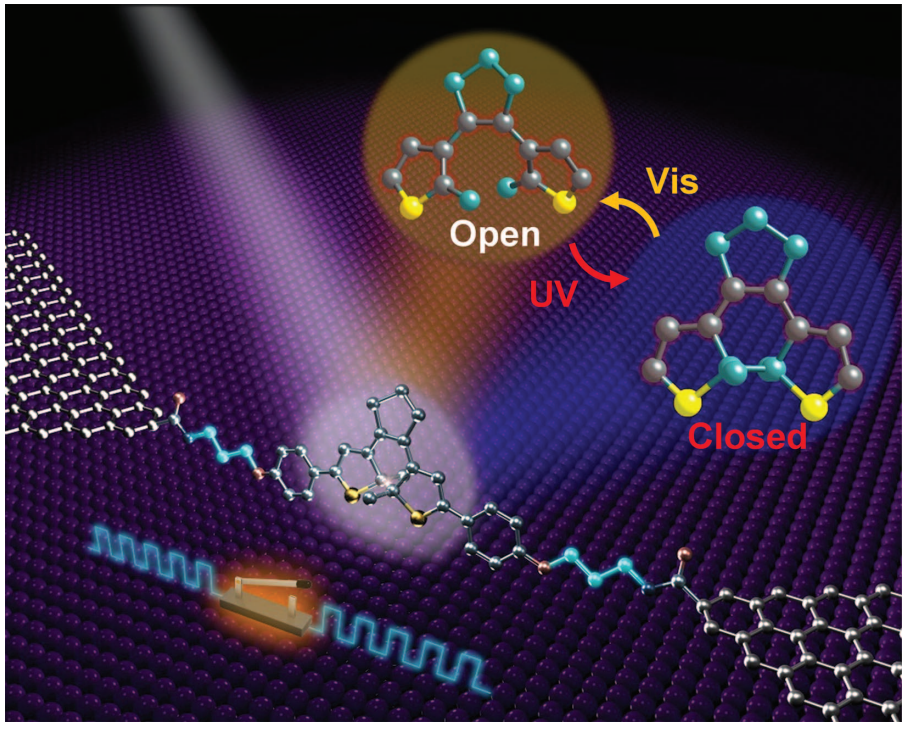

Fig. 1. Schematic of a graphene-diarylethene-graphene junction that highlights the expansion of the molecular bridge by methylene groups.

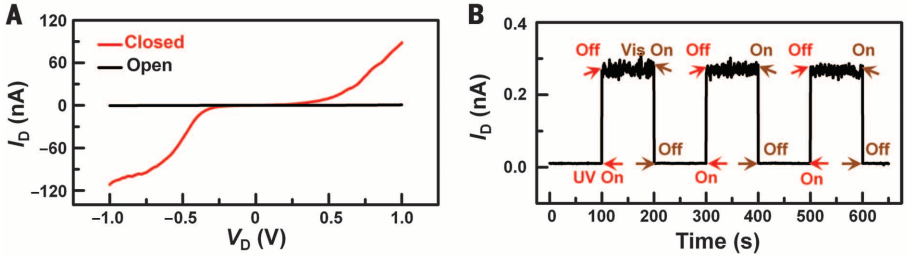

Fig. 2. Reversible photoswitching of graphene-diarylethene-graphene junctions. (**A**) *I-V* characteristics of individual diarylethenes in open (black line) and closed (red line) form at gate voltage V_G = 0 V. V_D, drain voltage; I_D, drain current. (**B**) Real-time measurement of the current through a diarylethene molecule that reversibly switches between the closed and open forms, upon exposure to ultraviolet (UV) and visible (Vis) radiation, respectively. V_D = 100 mV and V_G = 0 V.

in the bias range explored, thus enabling conduction. Assuming a charge-hopping transport mechanism, for the closed-ring molecular bridge at room temperature, our analysis establishes that the threshold bias voltage for the onset of appreciable current is in the range 0 to 0.38 V [as shown in supplementary materials, section S9.2 (*18*), this range is narrowed to 0 to 0.23 V if the computational uncertainties in the HOMO and reorganization energy are limited to the respective standard deviations]. Moreover, our theoretical analysis predicts a minimum threshold bias voltage of 1.2 V for observing appreciable conduction through the open molecular form. The theoretical predictions for both closed and open molecular forms are in agreement with the experimental current-voltage characteristics reported in Fig. 2A, where the onset of the current through the closed molecule occurs at ~0.3 V, whereas no appreciable conduction through the open molecule is observed up to 1 V. Assuming that tunneling mediated by a molecular level is at play and using the elegant theoretical approach by Bâldea *et al.* (*19*), we again find that the offset of the HOMO from the electrode Fermi level is significantly larger for the open form than for the closed form of the diarylethene bridge (fig. S8) (*18*).

If resonant tunneling (as is described by the Landauer-Büttiker formalism) is assumed as the dominant conduction mechanism, as was recently done for other diarylethene junctions (*20*), the threshold bias voltage for the onset of appreciable current is located in the range of 0.3 to 1.0 V, which is still compatible with the characteristics

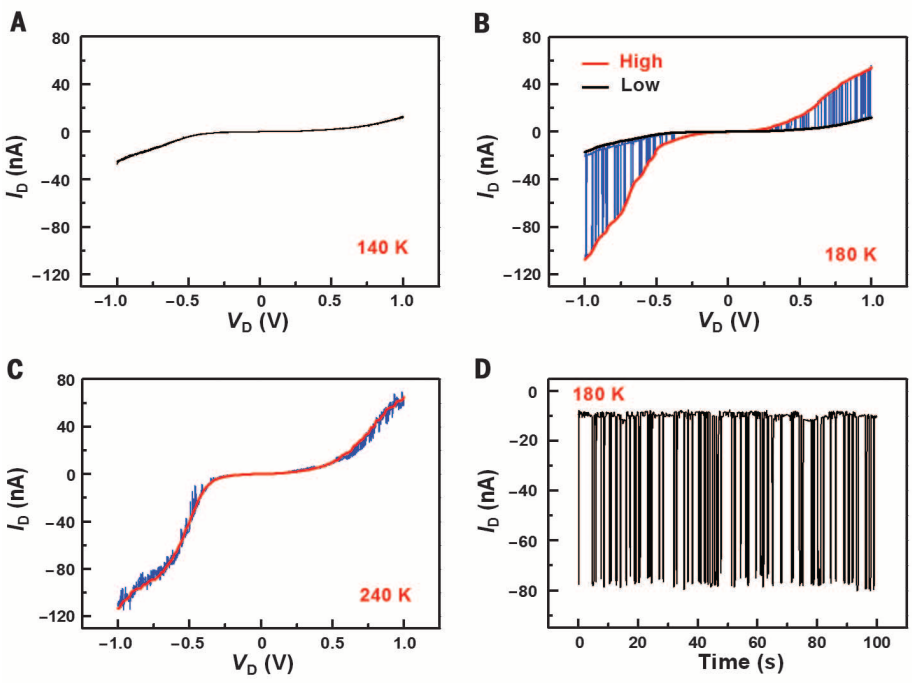

Fig. 3. Temperature-dependent stochastic switching of graphene-diarylethene-graphene junctions. (**A**) *I-V* characteristics of a single diarylethene junction in the closed form screened at 140 K for at least three times, which do not show stochastic switching. (**B**) Stochastic switching between two conductive states at 180 K. (**C**) *I-V* characteristics at 240 K. The stochastic conductance switching starts to disappear at this temperature. (**D**) Real-time recording of stochastic conductance switching at 180 K, with a source-drain bias of −0.8 V and a gate voltage of 0 V. The full details of the temperature-dependent stochastic conductance switching are provided in figs. S13 to S21 (*18*).

in Fig. 2A. A reliable discrimination between the hopping and resonant tunneling mechanisms for conduction requires further experimental and theoretical analysis (table S4 and its discussion) (*18*). In either mechanism, the energy gap between the molecular HOMO and the graphene Fermi level plays a crucial role in determining the threshold bias voltage for conduction, also because of the relatively small reorganization energy, which we have calculated to be $\lambda = (0.27 \pm 0.02)$ eV.

In addition to the photoinduced switching (Fig. 2B), systematic measurements over a wide temperature range revealed stochastic switching of the closed junction between two conductive modes (Fig. 3). This phenomenon was observed only for the closed form in the temperature range of 160 to 240 K (figs. S13 to S21 and tables S2 and S3) (*18*). Although the detailed mechanism of this behavior cannot be decided yet, some conclusions can be reached from our observations and theoretical analysis. This analysis indicates that neither the SOMO (singly occupied molecular orbital) of the molecular cation nor the LUMO of the neutral molecule are involved in this stochastic switching because these levels are much lower and higher in energy, respectively, than the unbiased graphene Fermi level (*21*, *22*). In either the hopping or the resonant tunneling model (*23*), the stochastic switching may be caused by a diarylethene conformational change, possibly driven by transient molecular charging—that is, changing occupation of the molecular HOMO—which is similar to that recently observed in organometallic single-molecule junctions with a redox center that is weakly coupled to the electrodes (*24*). Such a conformational change can lead to a bistable free-energy surface, with relative stability determined by entropy (number of microstates involved) and therefore sensitive to temperature. The current-voltage (*I-V*) characteristics in figs. S14 and S20 (*18*) are consistent with this picture if the two locally stable conformations have different conductions. In a simple model for such behavior—the polaron model of Galperin *et al.* (*23*)—the entropic term results in a temperature-dependent molecular electronic (free) energy, and the relative stability of the two conductive states predicted by the model is inverted as the temperature increases (fig. S27) (*18*). The current measurements do not rule out the possibility that stochastic conductance switching similar to that in Fig. 3 may be observed for the open-form molecular bridge at higher voltages for which the open-form HOMO enters the electrode Fermi window.

Both the photoswitching (Fig. 2) and the stochastic conductance switching (Fig. 3) were consistently observed in many devices for many switching cycles (more than 100 cycles for photoswitching and ~10^5 to 10^6 cycles for stochastic switching). Furthermore, the photoswitches produced in this work have been stable for over a year.

This work shows that molecules with suitable conductive properties and amenable to anchoring to solid-state electrodes can be key components for future nanoelectronics. Molecular engineering aimed to modulate the molecule-electrode coupling strengths has been the key to our success in constructing fully reversible, two-mode, single-molecule electrical switches.

REFERENCES AND NOTES

1. R. Naaman, *Phys. Chem. Chem. Phys.* **13**, 13153–13161 (2011).
2. A. K. Tatikonda, M. Tkachev, R. Naaman, *Biosens. Bioelectron.* **45**, 201–205 (2013).
3. S. Rochat, T. M. Swager, *ACS Appl. Mater. Interfaces* **5**, 4488–4502 (2013).
4. A. Migliore, R. Naaman, D. N. Beratan, *Proc. Natl. Acad. Sci. U.S.A.* **112**, E2419–E2428 (2015).
5. B. G. Mathapa, V. N. Paunov, *Biomater. Sci.* **2**, 212–219 (2014).
6. K. Famm, B. Litt, K. J. Tracey, E. S. Boyden, M. Slaoui, *Nature* **496**, 159–161 (2013).
7. M. T. Meredith, S. D. Minteer, *Annu. Rev. Anal. Chem.* **5**, 157–179 (2012).
8. *Nat. Nanotechnol.* **8**, 377–467 (2013).
9. M. Irie, *Chem. Rev.* **100**, 1685–1716 (2000).
10. B. K. Pathem, S. A. Claridge, Y. B. Zheng, P. S. Weiss, *Annu. Rev. Phys. Chem.* **64**, 605–630 (2013).
11. J. L. Zhang *et al.*, *Chem. Soc. Rev.* **44**, 2998–3022 (2015).
12. D. Dulić *et al.*, *Phys. Rev. Lett.* **91**, 207402 (2003).
13. A. C. Whalley, M. L. Steigerwald, X. Guo, C. Nuckolls, *J. Am. Chem. Soc.* **129**, 12590–12591 (2007).
14. C. Jia *et al.*, *Angew. Chem. Int. Ed.* **52**, 8666–8670 (2013).
15. C. Jia, X. Guo, *Chem. Soc. Rev.* **42**, 5642–5660 (2013).
16. X. Guo *et al.*, *Science* **311**, 356–359 (2006).
17. Y. Cao *et al.*, *Angew. Chem. Int. Ed.* **51**, 12228–12232 (2012).
18. Materials and methods are available as supplementary materials on *Science* Online.
19. I. Bâldea, Z. Xie, C. D. Frisbie, *Nanoscale* **7**, 10465–10471 (2015).
20. T. Sendler *et al.*, *Adv. Sci.* **2**, 1500017 (2015).
21. A. Migliore, A. Nitzan, *ACS Nano* **5**, 6669–6685 (2011).
22. A. Migliore, A. Nitzan, *J. Am. Chem. Soc.* **135**, 9420–9432 (2013).
23. M. Galperin, M. A. Ratner, A. Nitzan, *Nano Lett.* **5**, 125–130 (2005).
24. F. Schwarz *et al.*, *Nat. Nanotechnol.* **11**, 170–176 (2016).

ACKNOWLEDGMENTS

We acknowledge Z. Liu, N. Kang, J. Bergfield, and C. Van Dyck for insightful discussions. This work was supported by the National Basic Research Program of China (2012CB921404 and 2012CB932703) (X.G. and H.Q.X.), the National Natural Science Foundation of China (21225311, 91333102, 21373014, 21190033, 91221202, and 61321001) (X.G., D.-H.Q., and H.Q.X.), the Israel Science Foundation (A.N. and A.M.), the U.S.-Israel Bi-national Science Foundation (A.N.), and the University of Pennsylvania (A.N.).

SUPPLEMENTARY MATERIALS

www.sciencemag.org/content/352/6292/1443/suppl/DC1
Materials and Methods
Supplementary Text
Figs. S1 to S27
Databases S1 to S6
References (*25*–*51*)

5 March 2016; accepted 3 May 2016
10.1126/science.aaf6298

Science

Covalently bonded single-molecule junctions with stable and reversible photoswitched conductivity

Chuancheng Jia, Agostino Migliore, Na Xin, Shaoyun Huang, Jinying Wang, Qi Yang, Shuopei Wang, Hongliang Chen, Duoming Wang, Boyong Feng, Zhirong Liu, Guangyu Zhang, Da-Hui Qu, He Tian, Mark A. Ratner, H. Q. Xu, Abraham Nitzan, and Xuefeng Guo

Science, 352 (6292), • DOI: 10.1126/science.aaf6298

Stable molecular switches

Many single-molecule current switches have been reported, but most show poor stability because of weak contacts to metal electrodes. Jia *et al.* covalently bonded a diarylethene molecule to graphene electrodes and achieved stable photoswitching at room temperature (see the Perspective by Frisbie). The incorporation of short bridging alkyl chains between the molecule and graphene decoupled their pielectron systems and allowed fast conversion of the open and closed ring states.

Science, this issue p. 1443; see also p. 1394

Science (ISSN 1095-9203) is published by the American Association for the Advancement of Science. 1200 New York Avenue NW, Washington, DC 20005. The title *Science* is a registered trademark of AAAS.